J Electroceram (2009) 23:254–257
DOI 10.1007/s10832-008-9414-5

Improving the rate performance of $LiCoO_2$ by Zr doping

Seon Hye Kim · Chang-Sam Kim

Received: 30 May 2007 / Accepted: 4 January 2008 / Published online: 1 May 2008

Abstract Zr-doped $LiCoO_2$ cathode materials for lithium ion batteries were synthesized by an ultrasonic spray pyrolysis method. The synthesized powders with less than 1 mol% Zr had a single phase layered structure while those with 5 mol% Zr had a little secondary phase, Li_2ZrO_3. The cycle stabilities of Zr-doped and undoped $LiCoO_2$ were compared at various charge–discharge rates. The Zr-doped $LiCoO_2$ showed much improved cycle stability compared to the undoped, especially at a high C-rate of 3C (4.2 mA/cm^2). To investigate the reasons of the improvement, changes of the lattice parameters and the interatomic distances of Co–Co and Co–O of the doped and the undoped powders were analyzed using XRD and EXAFS. The lattice parameters, a and c, increased in the powders with less than 1 mol% Zr, but decreased in the powder with 5 mol% Zr. On the other hand, the interatomic distances of Co–Co and Co–O did not change with Zr doping. From these results, the improved cycle stability is thought to be due to the expanded inter-slab distance, which enhances Li-ion mobility during charge/discharge processes.

Keywords Lithium ion battery · Zirconium-doping · Rate performance · Slab distance · EXAFS

S. H. Kim · C.-S. Kim (✉)
Battery Research Center, KIST,
Seoul 130-650, Korea
e-mail: cskim@kist.re.kr

S. H. Kim
e-mail: netysh@hanmail.net

1 Introduction

Rechargeable lithium ion batteries for hybrid electric vehicles (HEV) or for power tools require high charge and discharge rates. Therefore, the cathode materials for high-rate capability of lithium ion batteries have attracted growing attention recently [1, 2]. $LiCoO_2$ with layered structure is the earliest found cathode material, but it has some disadvantages. Metallic cobalt is very expensive and toxic [3, 4]. The crystalline structure of $LiCoO_2$ is distorted irreversibly due to the dissolution of lattice oxygen at highly delithiated states and becomes unstable at high temperatures [5]. Recently, attempts for improving the stability of $LiCoO_2$ by means of doping and coating with some inactive metals have shown positive results in not only capacity and cycle stability but also high-rate performance [6–11]. Xu et al. [12] reported that both Zr and Mg doping increased the capacity and stability of $LiCoO_2$. Kim et al. [11] reported that the doping led to an increase of $LiCoO_2$ lattice parameters, a and c, due to the larger ion size of Mg^{2+} or Zr^{4+} compared to that of Co^{3+}. They suggested that some Mg^{2+} and Zr^{4+} ions might locate at the inter-slab space because they were as large as Li^+ ion, which resulted in improved rate performance and prevented the distortion of structure during charge and discharge processes. However, the reason of lattice expansion has not been clearly understood yet.

In this study, $Li(Co_{1-x}Zr_x)O_2$ (x=0, 0.005, 0.01, 0.05) was prepared via ultrasonic spray pyrolysis method by which homogeneous compounds with little amount of dopants could be prepared easily. Particular attention was paid to the variation of c-rate performance at high voltage, 4.5 V. Microstructure and crystal structure were analyzed using SEM and XRD. The interatomic distances of Co–Co

and Co–O were estimated using extended X-ray absorption fine structure spectroscopy (EXAFS).

2 Experimental procedure

$Li(Co_{1-x}Zr_x)O_2$ was synthesized using an ultrasonic spray pyrolysis (USP) method with $LiNO_3$, $Co(NO_3)_2{\cdot}6H_2O$ and $ZrO(NO_3)_2{\cdot}xH_2O$ (99.5, Aldrich, USA). Relevant amounts of Li, Co and Zr nitric salts were dissolved in deionized water to be the concentration of 0.5 mol/l. The aqueous solution was atomized using an ultrasonic nebulizer with a resonant frequency of 1.67 MHz. The aerosol stream was introduced into the vertical quartz reactor with two heating zones of 400 and 800 °C, respectively. Synthesized powders were calcined at 900 °C for 20 h in air.

The crystal structures of $Li(Co_{1-x}Zr_x)O_2$ were characterized by XRD (Model D/Max-3A, Rigaku, Japan). EXAFS measurements were performed in transmission mode at beam 7C1 of Pohang light source (PLS) using a Si(111) double-crystal monochromator. Calibration was carried out prior to all measurements using the first inflection point of the spectrum of Co foil, i.e. Co K-edge=7709 eV, as a reference. The morphology of powders was analyzed with SEM(Model L-240, Hitachi, Japan).

The active materials, acetylene black and polyvinylidene difluoride with a ratio of 90:5:5 wt% were mixed with NMP using a solder paste mixer. Coin type (type 2032) half-cells with lithium foil as a counter electrode were assembled. $LiPF_6$ of 1 M in a mixture of ethylene carbonate/dimethyl carbonate/ethylmethyl carbonate of a 1:1:1 volume ratio was used as electrolyte, and polypropylene-based film as a separator. The charge–discharge characteristics of cells were galvanostatically tested with a battery cycler (WBC 3000, Won A Tech, Korea) in a voltage range of 3.0~4.2 V and 3.0–4.5 V vs Li/Li^+.

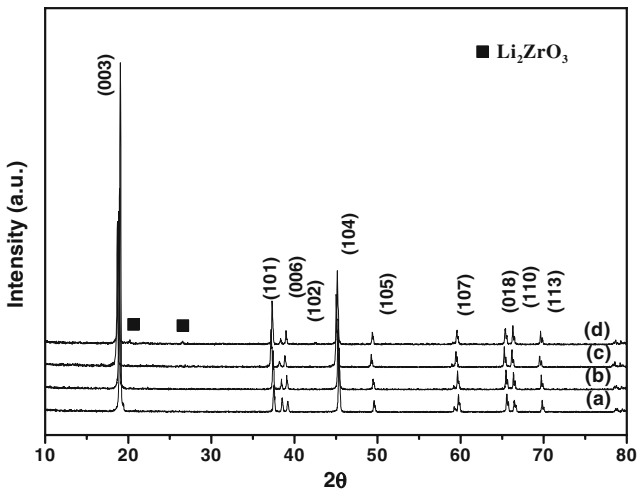

Fig. 1 XRD patterns of (**a**) $LiCoO_2$, (**b**) $LiCo_{0.995}Zr_{0.005}O_2$, (**c**) $LiCo_{0.99}Zr_{0.01}O_2$, (**d**) $LiCo_{0.95}Zr_{0.05}O_2$ powders heat-treated at 900 °C for 20 h. Secondary phase, Li_2ZrO_3, appears only at (**d**)

Table 1 Structural parameters of $Li(Co_{1-x}Zr_x)O_2$ powders.

	a lattice	c lattice	I_{003}/I_{104}
Bare	2.8060	14.0204	5.635
Zr0.005	2.8150	14.0378	2.836
Zr0.01	2.8271	14.0991	2.001
Zr0.05	2.8209	14.0673	1.797

3 Results and discussion

Figure 1 shows XRD patterns of $Li(Co_{1-x}Zr_x)O_2$ ($0 \le x \le 0.05$) synthesized using an ultrasonic spray pyrolysis and subsequently calcined at 900 °C for 20 h. It shows well separated peaks around 37° and 64° to be identified as (006)/(102) and (018)/(110) respectively, which are characteristic of the layered structure of $R\bar{3}m$ hexagonal α-$NaFeO_2$ structure. The synthesized $Li(Co_{1-x}Zr_x)O_2$ powders in which x was less than 0.01 show layered structure of single phase HT-$LiCoO_2$ type. However, the secondary phase, Li_2ZrO_3, was identified in the $Li(Co_{0.95}Zr_{0.05})O_2$. Lattice parameters, a and c, and peak intensity ratio, $I_{(003)}/I_{(104)}$, are summarized in Table 1.

As increasing Zr doping, the lattice parameters, a and c, increased except $Li(Co_{0.95}Zr_{0.05})O_2$ which had the secondary phase. It was reported that the doping of larger ions than Co ion increased lattice parameters of $LiCoO_2$ [11–13]. The ionic radii of ions with six-coordination are Li^+ (0.90 Å), Zr^{4+} (0.86 Å), Co^{3+} (0.685 Å) and Co^{4+} (0.67 Å). So the results of lattice expansion in this study correspond to those of others. The layered structure of $LiCoO_2$, in which the Li^+ and Co^{3+} ions occupy the alternate (111) planes of the rock salt structure to give a layer sequence of O–Li–O–Co–O– along the c axis. The layered structure with covalently bonded CoO_6 octahedra layers, i.e. cobalt-slab, allows a reversible extraction/insertion of lithium ions from/into lithium layers, i.e. inter-slab. However, it is difficult to estimate using XRD whether the lattice expansion is caused by an expansion of cobalt-slab or by that of inter-slab because of the low atomic scattering factor of lithium.

Figure 2 shows the X-ray absorption near edge structure (XANES) at the Co K-edge. There are two weak absorption peaks at ~7,710 eV (peak A) and ~7,718 eV (peak B), and a strong absorption peak at ~7,727 eV (peak C). The A peak corresponds to the transition of the 1s electron to an unoccupied $3d$–e_g orbital of Co^{3+} ion. The B and C peaks are the result of the transition of the 1s electron to 4p with the shakedown process by ligand to metal charge transfer

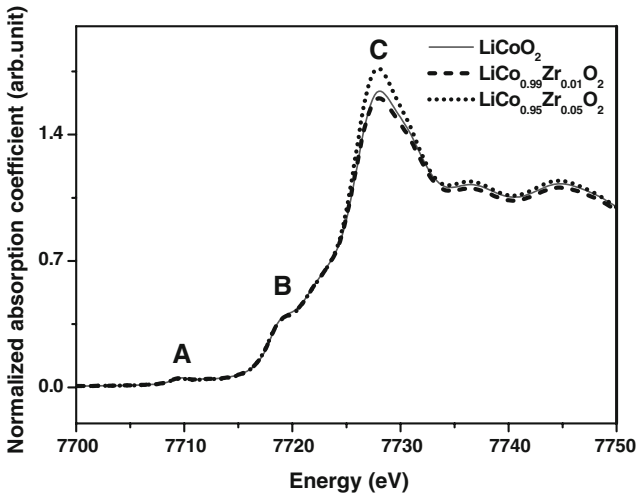

Fig. 2 Normalized Co K-edge XANES of $Li(Co_{1-x}Zr_x)O_2$ with various amount of Zr

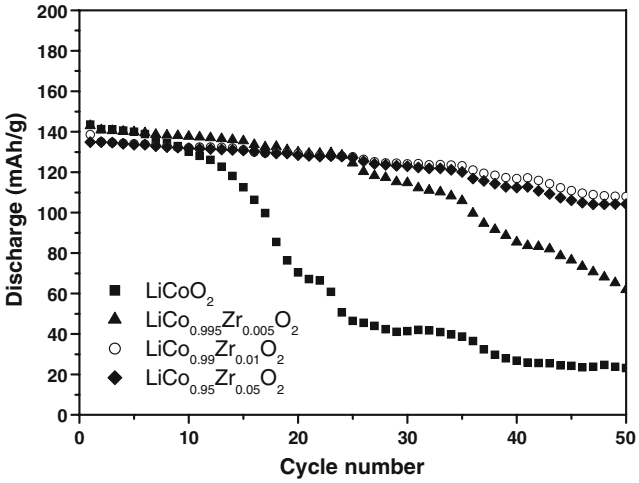

Fig. 4 Discharge capacity as a function of cycle numbers for cells operated at 1C (1.4 mA/cm^2) in the voltage range of 3.0–4.2 V

and without the shakedown process, respectively. The intensity of A and B peaks are closely related to the local distortion of CoO_6 octahedral symmetry. The C peak is related to the oxidation state of Co ion. Changes are hardly observed in the A and B peaks. This indicates that the Zr doping does not give rise to a distortion of the crystalline structure. In the C peak, a slight shift to the lower energy side is observed in the Zr doped materials compared to the undoped. This shift is due to slightly reduced oxidation state of the Co ions.

Figure 3 shows Fourier transform magnitudes of the Co K-edge EXAFS spectra of the Zr doped and the undoped powders. The first peak at ~1.46 Å and the second peak at ~2.34 Å indicating the interatomic distance are due to Co–O and Co–Co interaction respectively. The peak intensity and width are related with thermal fluctuations and local order. It can be found that they do not exhibit any changes in their positions by Zr doping, indicating no local structural changes around Co atoms. This is very consistent with the result of XANES. From the result of XRD, the increase of lattice parameters of Zr doped $LiCoO_2$ was found. The layered structure of $LiCoO_2$ is the alternative stack of cobalt-slabs and inter-slabs. Because the expansion of cobalt-slab was not recognized from the results of EXAFS, it could be thought that the increase of the lattice parameters of Zr doped $LiCoO_2$ was caused by the expansion of inter-slab.

Figure 4 shows the cyclic performances of cells in the voltage range of 3.0–4.2 V at room temperature. At first cycle, cells were charged and discharged at C/10 (0.14 mA/cm^2) and at the following cycles at 1C (1.4 mA/cm^2). The initial discharge capacities of 144, 143, 139 and 135 mAh/g were obtained with increasing x, 0, 0.05, 0.01 and 0.05 in $Li(Co_{1-x}Zr_x)O_2$. The discharge capacities of Zr doped

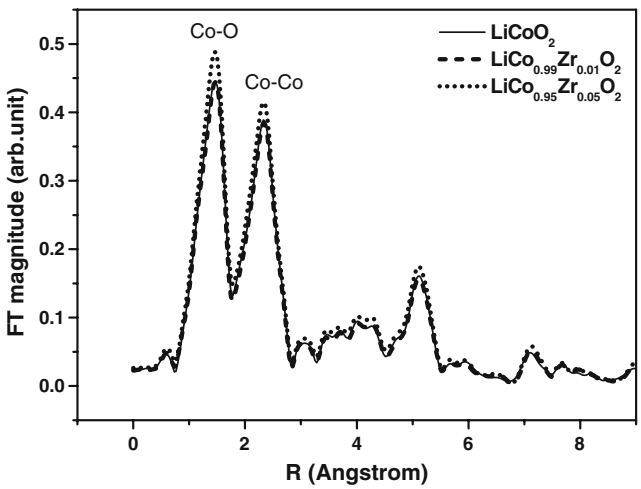

Fig. 3 FT magnitude of Co K-edge κ^3-weighted EXAFS spectra as a function of interatomic distance for $Li(Co_{1-x}Zr_x)O_2$ with various amount of Zr

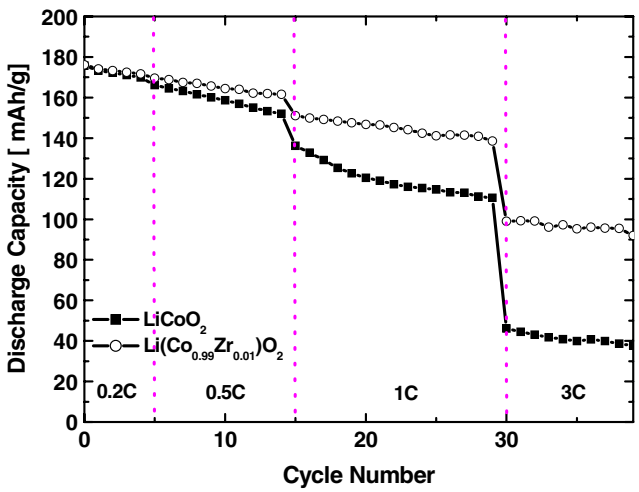

Fig. 5 Discharge curves of bare and $Li(Co_{0.99}Zr_{0.01})O_2$ at the different discharge rates from 0.2C to 3C in the voltage of 3.0~4.5 V

samples with 1 and 5 mol% were 108 and 104 mAh/g after 50 cycles, respectively. Meanwhile, the discharge capacity of undoped sample started to decrease drastically only after 10 cycles and then dropped down to 23 mAh/g after 50 cycles. Figure 5 shows the change of discharge capacities of $LiCoO_2$ and $Li(Co_{0.99}Zr_{0.01}O_2)$ at the different discharge rates from 0.2C to 3C in the voltage of 3.0 ~4.5 V. The first discharge capacities are 175 and 176 mAh/g for $LiCoO_2$ and $Li(Co_{0.99}Zr_{0.01})O_2$, respectively. It is noticeable that Zr doping shows the same initial capacity as undoped in spite of Zr ion dose not contribute to redox reaction during charge/discharge processes. The Zr doped sample shows much more improved rate performance than the undoped. It is obvious that Zr doping significantly improves both a cycling stability and a rate performance especially at higher discharge current densities. These improvements might be caused by higher lithium ion mobility during charge/discharge processes, which is due to the expansion of inter-slab distance.

4 Summary

The Zr doped $Li(Co_{1-x}Zr_x)O_2$ powders were synthesized via ultrasonic spray pyrolysis. The lattice parameters and inter-atomic distances of Co–O and Co–Co of synthesized powders were compared with each other. The cycle stability and C-rate performance of synthesized powders were also estimated using 2032 type coin cells. The solubility limit of Zr in $LiCoO_2$ was ~1 mol% in this work. The more addition of Zr than 1 mol% gave rise to the formation of secondary phase, Li_2ZrO_3. As the Zr doping, the lattice parameters of $Li(Co_{1-x}Zr_x)O_2$ increased up to x=0.01. However, the inter-atomic distances of Co–O and Co–Co were not changed by Zr doping. From the results of XRD and EXAFS, the lattice expansion in Zr doped $LiCoO_2$ was deduced by the expansion of LiO_6 octahedra that composed the inter-slabs. The cycle stability and C-rate performance were significantly improved by Zr doping up to x=0.01, without sacrificing the initial capacity. These improved cycle stability and C-rate performance might be due to the expansion of inter-slab distance, which makes the extraction/insertion of Li ions easy during charge/discharge processes.

Acknowledgement The authors are grateful for the financial support from KIST (Korea Institute of Science and Technology) and to the authorities of PLS (Pohang Light Source) for X-ray absorption spectroscopic measurements.

Reference

1. H.Y. Liang, X.P. Qiu, H.L. Chen, Z.Q. He, W.T. Zhu, L.Q. Chen, Electrochem. Commun. **6**, 789 (2004)
2. K.M. Abraham, D.M. Pasquariello, E.M. Willstaedt, J. Electrochem. Soc. **145**, 482 (1998)
3. H.F. Gibbard, J. Power Sources. **26**, 81 (1989)
4. T. Nagura, K. Tazawa, Prog. Batteries Sol. Cells. **9**, 20 (1990)
5. S.T. Myung, N. Kumagai, S. Komaba, H.T. Chung, Solid State Ionics. **139**, 47 (2001)
6. Y.J. Kim, T.J. Kim, J.W. Shin, B. Park, J. Cho, J. Electrochem. Soc. **49**(10), A1337 (2002)
7. J. Cho, C.S. Kim, S.I. Yoo, Electrochem. Solid-State Lett. **3**(8), 362 (2000)
8. Z. Wang, C. Wu, L. Liu, F. Wu, L. Chen, X. Huang, J. Electrochem. Soc. **149**, A466 (2002)
9. Z. Chen, J.R. Dahn, Electrochem. Solid-State Lett. **5**(10), A213 (2002)
10. S. Huang, Z. Wen, X. Yang, Z. Gu, X. Xu, J. Power Sources. **148**, 72 (2005)
11. H.S. Kim, T.K. Ko, B.K. Na, W.I. Cho, B.W. Cho, J. Power Sources. **138**, 232 (2004)
12. H.Y. Xu, S. Xie, C.P. Zhang, C.H. Chen, J.Power Sources. **148**, 90 (2005)
13. S. Levasseur, M. Menetrier, C. Delmas, Chem. Mater. **14**, 3584 (2002)